2-Thia-1,3,5-triaza-7-phosphaadamantane 2,2-Dioxide ($PASO_2$). Comparative Structural and Reactivity Investigation with the Water-Soluble Phosphine Ligand 1,3,5-triaza-7-phosphaadamantane (PTA)

Donald J. Darensbourg,* Jason C. Yarbrough, and Samuel J. Lewis

Department of Chemistry, Texas A&M University, College Station, Texas 77843

Received January 14, 2003

The derivative 2-thia-1,3,5-triaza-phosphaadamantane 2,2-dioxide ($PASO_2$) has been characterized by spectroscopy and by X-ray crystallography. Unlike its PTA (1,3,5-triaza-7-phosphaadamantane) analogue, replacement of a $-CH_2-$ unit in PTA with $-SO_2-$ renders $PASO_2$ largely insoluble in water at ambient temperature (<0.70 g/L vs 236 g/L for PTA). This latter property makes it of no use as a water-solubilizing ligand for organometallic complexes. Interestingly, alkylation of $PASO_2$ with methyl iodide occurs quantitatively at the phosphorus center to afford the iodide salt. This derivative has also been characterized by X-ray crystallography and $^1H/^{31}P$ NMR spectroscopy, where the ^{31}P resonance was observed to be shifted downfield relative to $PASO_2$ (−39.2 vs −115.9 ppm). Although PTA has long been thought to react with methyl iodide to provide exclusively a monoalkylated product at one of the nitrogen centers, a close examination of this process via ^{31}P NMR spectroscopy has shown monomethylation to take place at both nitrogen and phosphorus, with the latter being the minor product. Computational studies (DFT and HF) were performed in an effort to explain this difference in reactivity; however, no definitive conclusions could be reached from these calculations. Comparative studies (based on CO stretching frequencies and force constants) of group 6 metal carbonyl derivatives of PTA and $PASO_2$ showed these ligands to be electronically extremely similar. This conclusion was supported by the bonding parameters determined in $W(CO)_5PTA$ and $W(CO)_5PASO_2$ complexes by X-ray crystallography.

Introduction

In 1973, Chatt and co-workers performed transition-metal-catalyzed reactions in water.[1] Since then, there has been a tremendous effort in the development of new water-soluble organotransition-metal complexes with the practical and environmental benefits in mind. This is principally accomplished through ligand design; thus, a variety of water-soluble ligand systems has been developed and explored. The most successful and noted of these systems have been phosphines with water-soluble substituents, such as sulfonated aryl groups,[2] ammonium groups,[3] and carboxylated aromatic groups.[4] Further, there has been much success with some non-aromatic groups such as tris(hydroxymethyl)phosphine ($P(CH_2OH)_3$).[5,6] Another nonionic aliphatic water-soluble phosphine is the tetrabasic 1,3,5-triaza-7-phosphaadamantane (PTA), as shown in Chart 1. Due to its utility as a water-soluble ligand and in efforts to explore the unique chemistry of this ligand, our group has been active in the investigation of the different facets of PTA.[7−13] Further, PTA has been investigated in many different areas such as photoluminecence of gold(I) phosphine complexes[14−18] and intermolecular hydrogen−metal interactions,[19] as well as its use as a precursor

(1) Chatt, J.; Leigh, G. J.; Slade, R. W. *J. Chem. Soc., Dalton Trans.* **1973**, 2021.
(2) (a) Herrmann, W. A.; Kellner, J.; Riepl, H. *J. Organomet. Chem.* **1990**, *389*, 103. (b) Toth, Z.; Joó, F.; Beck, M. T. *Inorg. Chem. Acta* **1980**, *42*, 153.
(3) Mohr, B.; Lynn, D. M.; Grubbs, R. H. *Organometallics* **1996**, *15*, 4317.
(4) Hoots, J. E.; Rauchfuss, T. B.; Wrobleski, D. A. *Inorg. Synth.* **1982**, *21*, 175.
(5) Ellis, J. W.; Harrison, K. N.; Hoye, P. A. T.; Orpen, A. G.; Pringle, P. G.; Smith, M. B. *Inorg. Chem.* **1992**, *31*, 3026.
(6) Hoye, P. A. T.; Pringle, P. G.; Smith, M. B.; Worboys, K. *J. Chem. Soc., Dalton Trans.* **1993**, 269.
(7) Darensbourg, D. J.; Beckford, F. A.; Reibenspies, J. H. *J. Cluster Sci.* **2000**, *11*, 95.
(8) Darensbourg, D. J.; Robertson, J. B.; Larkins, D. L.; Reibenspies, J. H. *Inorg. Chem.* **1999**, *38*, 2473.
(9) Darensbourg, D. J.; Stafford, N. W.; Joó, F.; Reibenspies, J. H. *Organomet. Chem.* **1995**, *488*, 99.
(10) Joó, F., Nadasdi, L.; Benyei, A. C.; Darensbourg, D. J. *J. Organomet. Chem.* **1996**, *512*, 45.
(11) Darensbourg, D. J.; Decuir, T. J.; Stafford, N. W.; Robertson, J. B.; Draper, J. D.; Reibenspies, J. H. *Inorg. Chem.* **1997**, *36*, 4218.
(12) Darensbourg, D. J.; Joó, F.; Kannisto, M.; Kathó, A.; Reibenspies, J. H. *Organometallics* **1992**, *11*, 1990.
(13) Darensbourg, D. J.; Joó, F.; Kannisto, M.; Kathó, A.; Reibenspies, J. H.; Daigle, D. J. *Inorg. Chem.* **1994**, *33*, 200.
(14) Forward, J. M.; Assefa, Z.; Fackler, J. P. *J. Am. Chem. Soc.* **1995**, *117*, 9103.
(15) Forward, J. M.; Fackler, J. P.; Staples, R. J. *Organometallics* **1995**, *14*, 4195.
(16) Forward, J. M.; Assefa, Z.; Staples, R. J.; Fackler, J. P. *Inorg. Chem.* **1996**, *35*, 16.
(17) Assefa, Z.; McBurnett, B. G.; Staples, R. J.; Fackler, J. P. *Inorg. Chem.* **1995**, *34*, 4965.
(18) Assefa, Z.; McBurnett, B. G.; Staples, R. J.; Fackler, J. P. *Inorg. Chem.* **1995**, *34*, 75.
(19) Alyea, E. C.; Ferguson, G.; Kannan, S. *Chem. Commun.* **1998**, 345.

10.1021/om0300225 CCC: $25.00
Publication on Web 04/17/2003

Chart 1

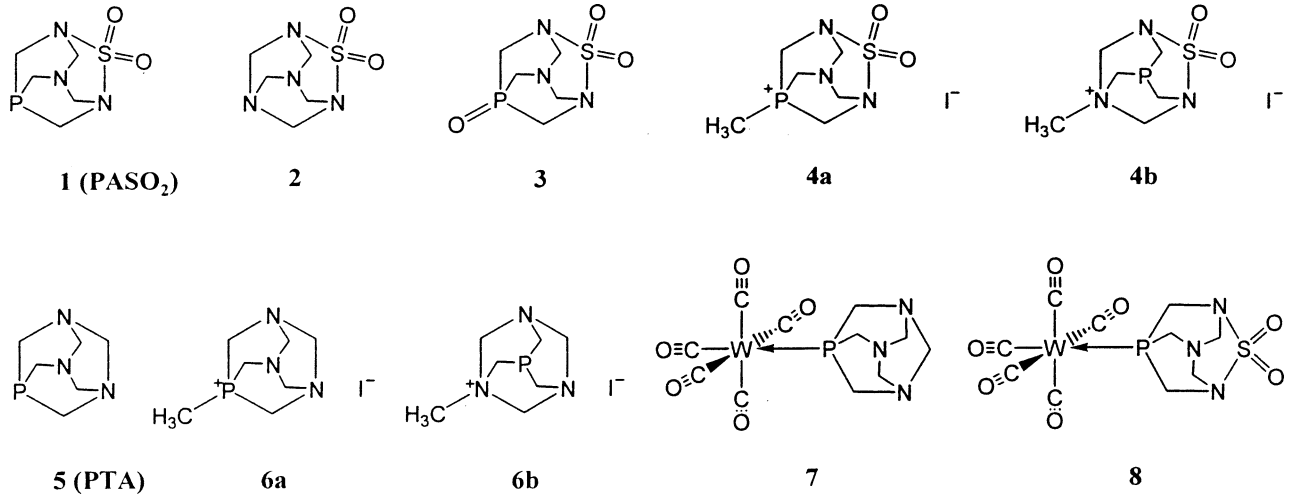

to other novel phosphine amine compounds and ligands.[20−23]

Our interest in the phosphaadamantyl motif has led us to focus attention on another derivative, 2-thia-1,3,5-triaza-7-phosphaadamantane 2,2-dioxide ($PASO_2$). This is illustrated in Chart 1 as compound **1**. The synthesis of this compound was reported by Daigle et al. in 1974 as part of an ongoing study into flame-retardant materials.[24] Unlike PTA, very few studies of compound **1** followed this initial report.[25] We have examined this compound as to its water solubility, coordination chemistry, oxidation, and alkylation, which we report herein, along with the structural characterization of $PASO_2$ and its derivatives by X-ray crystallography.

Experimental Section

All solvents were dried and deoxygenated by distillation from the appropriate reagent under a nitrogen atmosphere. Infrared spectra were recorded on a Mattson 6022 spectrometer with DTGA and MCT detectors. Routine IR spectra were collected using a 0.10 mm CaF_2 cell. Sulfamide, formaldehyde, tetrakis(hydroxymethyl)phosphonium chloride (THPC), hexamethylenetetraamine, and methyl iodide were purchased from the Aldrich Chemical Co. and used without further purification. The syntheses of 2-thia-1,3,5-triaza-7-phosphaadamantane 2,2,7-trioxide (O=$PASO_2$; **3**), 1-thia-2,4,6-triaza-8(6)-methyl-8-phosphaadamantane 1,1-dioxide iodide (**4**), PTA (**5**), Me-PTA iodide (**6**), and $W(CO)_5$PTA (**7**) were carried out as described in the literature.[24,26,27] Compound **3**: ^{31}P NMR (δ, ppm; DMSO) −16.63. Compound **4**: ^{31}P NMR (δ, ppm; D_2O) −39.17 (P−Me) and −109.06 (P−CH_2NMe). Compound **5**: ^{31}P NMR (δ, ppm; D_2O) −97.96. Compound **6**: ^{31}P NMR (δ, ppm; D_2O) −85.87 (N−CH_3) and −39.33 (P−CH_3). Compound **7**: ^{31}P NMR (δ, ppm; $CDCl_3$) −78.20.

Synthesis of $PASO_2$ (1). The preparation of compound **1** also follows the literature.[24] However, some modifications were made; hence, we report the details of the procedure here. Into an 80 mL beaker, 4.76 g (25 mmol) of THPC was delivered along with approximately 15 mL of ice-cold water (<5 °C). To the resulting clear solution was slowly added 1.28 g of NaOH (approximately 32 mmol) in a 50% (w/w) solution with stirring. After the solution was warmed to room temperature, 21.6 mL of a 37% formaldehyde solution was delivered, followed by addition of 2.4 g (25 mmol) of sulfamide and 3.8 g (25 mmol) of hexamethylenetetraamine at once. As these two components dissolved into the reaction solution, there was a slight elevation in temperature observed, and over the next 24 h a precipitate formed. The solid was collected by vacuum filtration. Dissolution of the solid into three 30 mL acetone washes followed by removal of the solvent under vacuum yielded 1.3 g (25% yield) of crude **1**. X-ray-quality crystals were grown directly from the reaction mixture over a 3 day period. Anal. Calcd for $C_5H_{10}N_3O_2PS$: C, 28.98; H, 4.83; N, 20.3. Found: C, 29.13, H, 4.76; N, 20.1. ^{31}P NMR (DMSO): δ −115.9 ppm.

Synthesis of $N_4(CH_2)_5SO_2$ (2). A 9 mL portion of 30% aqueous ammonia was added to 10 mL of water in a 100 mL beaker. To this solution was added 20 mL of formaldehyde and 2.5 g of sulfamide with vigorous stirring. The reaction mixture was stirred for 3 h or until a precipitate formed. The white precipitate was collected by filtration and washed with three 10 mL portions of water. Removal of the solid sample from the filter was achieved by dissolution in ∼15 mL of acetone. The solvent was removed under reduced pressure and dried overnight in vacuo to afford 2.82 g of product (57.0% yield). Anal. Calcd for $C_5H_{10}N_4O_2S$: C, 31.57; H, 5.30; N, 29.45. Found: C, 27.9; H, 4.90; N, 27.3. ^{1}H NMR (δ, ppm; acetone): 5.02 (d, 8H, $-NCH_2NSO_2-$), 5.18 (d, 2H, $CNCH_2NC$), ^{13}C NMR (δ, ppm; DMSO): 72.6 (s, 4C, SO_2-NCH_2N-), 71.7 (s, 1C, $CNCH_2NC$). X-ray-quality crystals were obtained by slow evaporation of an acetone solution of **2**.

Synthesis of $W(CO)_5PASO_2$ (8). In a 100 mL Schlenk flask charged with $W(CO)_6$ (2.0 mmol) and trimethylamine *N*-oxide (2.0 mmol), 30 mL of acetonitrile was added. The resulting yellow solution was stirred for 2 h at room temperature. After stirring, the reaction mixture was delivered into a 100 mL round-bottom flask fitted with a reflux condenser and containing $PASO_2$ (2.1 mmol). At this point the solution was heated to reflux for 1.5 h. The solvent was removed under vacuum, and the yellow solid was washed with cold hexane and cold water followed by recrystallization from hexane. ^{31}P NMR (δ, ppm): −81.6 (J^{183}_{W-31P} = 228.9 Hz). Anal. Calcd for $C_{10}H_{10}O_7N_3PSW$: C, 22.62; H, 1.90; N, 7.91. Found: C, 22.8; H, 1.85; N, 7.78.

Water Solubility. A 25 mL portion of water was added dropwise to 17.5 mg of **1** at room temperature with stirring.

(20) Nadasdi, L. Joó, F. *Inorg. Chem. Acta* **1999**, *293*, 218.
(21) Assmann, B.; Angermaier, K.; Paul, M.; Reide, J.; Schmidbauer, H. *Chem. Ber.* **1995**, *128*, 891.
(22) Daigle, D. J.; Pepperman, A. B. *J. Heterocycl. Chem.* **1975**, *12*, 579.
(23) Daigle, D. J.; Boudreaux, G. J.; Vail, S. L. *J. Chem. Eng. Data* **1976**, *21*, 240.
(24) Daigle, D. J.; Pepperman, A. B.; Boudreaux, G. *J. Heterocycl. Chem.* **1974**, *11*, 1085.
(25) Delerno, J. R.; Majeste, R. J.; Trefonas, L. M. *J. Heterocycl. Chem.* **1976**, *13*, 757.
(26) Daigle, D. J. *Inorg. Synth.* **1998**, *32*, 40−45.
(27) Darensbourg, M. Y.; Daigle, D. J. *Inorg. Chem.* **1975**, *14*, 1217.

Table 1. Crystallographic Data and Data Collection Parameters

	1	2	3	4a,b	7	8
empirical formula	$C_5H_{10}N_3O_2PS$	$C_5H_{10}N_4O_2S$	$C_5H_{10}N_3O_3PS$	$C_6H_{13}IN_3O_2PS$	$C_{11}H_{12}N_3O_5PW$	$C_{10}H_{10}N_3O_7PSW$
fw	207.22	190.23	223.19	349.12	481.06	531.09
space group	$P2_1/n$	$P2_1/n$	$P2_1/c$	$P2_1/n$	$P2_1/c$	$P2_1/c$
V (Å^3)	829.27(13)	774(2)	823.62(14)	2304.1(4)	1440.50(15)	1518.9(19)
Z	4	4	4	8	2	4
D_{calcd} (Mg/m^3)	1.660	1.632	1.800	1.212	1.109	1.161
a (Å)	6.0733(6)	6.332(10)	6.4904(6)	17.7505(17)	12.3379(7)	12.330(9)
b (Å)	12.3949(11)	11.649(18)	6.7429(7)	7.3185(7)	9.6838(6)	10.494(8)
c (Å)	11.3141(10)	10.553(16)	18.8694(18)	18.0238(18)	12.3083(15)	12.041(9)
β (deg)	103.179(2)	95.97(3)	94.166(2)	100.247(2)	101.6060(10)	102.873(11)
T (K)	110(2)	110(2)	110(2)	110(2)	110(2)	110(2)
μ(Mo Kα) (mm^{-1})	0.561	0.382	0.564	6.158	4.4077	7.887
wavelength (Å)	0.710 73	0.710 73	0.710 73	0.710 73	0.710 73	0.710 73
R_F (%)[a]	4.32	5.41	5.65	3.54	5.38	4.98
R_{wF} (%)[a]	11.75	14.63	13.22	9.36	14.38	12.61

[a] $R_F = \sum||F_o| - |F_c||/\sum F_o$ and $R_{wF} = \{[\sum w(F_o - F_c)^2]/\sum wF_o^2\}^{1/2}$.

A significant fraction of compound **1** was left undissolved as stirring was continued for an additional 1 h. Thus, the solubility in water at room temperature was $<7.0 \times 10^{-4}$ g/mL.

X-ray Crystallography. A Bausch and Lomb 10× microscope was used to identify suitable crystals of **1**−**4** and **6** from a representative sample of crystals. The crystals were coated in a cryogenic protectant (i.e. mineral oil and Apiezon grease) and fixed to a glass fiber. The mounted crystals were placed in a cold nitrogen stream (Oxford) maintained at 110 K on a Bruker SMART 1000 three-circle goniometer.

Crystal data and details of data collection from these samples are provided in Table 1. The X-ray data were collected on a Bruker CCD diffractometer and covered more than a hemisphere of reciprocal space by a combination of three sets of exposures; each exposure set had a different φ angle for the crystal orientation, and each exposure covered 0.3° in ω. The crystal-to-detector distance was 4.9 cm. Crystal decay was monitored by repeating the data collection for 50 initial frames at the end of the data set and analyzing the duplicate reflections; crystal decay was negligible. The space group was determined on the basis of systematic absences and intensity statistics.[28]

The structures were solved by direct methods. Full-matrix least-squares anisotropic refinement for all non-hydrogen atoms yielded $R(F)$ and $R_w(F^2)$ values as indicated in Table 1 at convergence. Hydrogen atoms were placed in idealized positions with isotropic thermal parameters fixed at 1.2 or 1.5 times the value of the attached atom. Neutral atom scattering factors and anomalous scattering factors were taken from Volume C of the International Tables for X-ray Crystallography.

For all the title compounds: data reduction, SAINTPLUS (Bruker[29]); program(s) used to solve the structure, SHELXS-86 (Sheldrick[30]); program(s) used to refine the structure, SHELXL-97 (Sheldrick[31]); program(s) used for molecular graphics, SHELXTL version 5.0 (Bruker[32]); software used to prepare material for publication, SHELXTL version 5.0 (Bruker[32]).

Calculations. Theoretical calculations were utilized in order to obtain insight into the differences between PTA and $PASO_2$ in terms of their reactivities toward alkylation. Full geometry optimizations were performed by starting with the crystal structure for compound **1** and making appropriate modifications to generate structures for **4a**,**b**, **5**, and **6a**,**b** (as shown in Chart 1) and employing ab initio methodologies. Hartree−Fock (HF) and density functional theory (DFT) optimizations were performed using the D95*[33] and 6-31G[34] basis sets. DFT calculations were carried out using Becke's three-parameter hybrid method[35] coupled to the correlation functional of Lee, Yang, and Parr (B3LYP).[36] All calculations were carried out using the Gaussian 98 software package[37] on Titan running at the Laboratory for Molecular Simulation at Texas A&M University.

Results and Discussion

Synthesis and Characterization of Compound 1. The reaction of THP (tris(hydroxymethyl)phosphine), hexamethylenetetraamine, sulfamide, and excess formaldehyde in water resulted in the precipitation of a colorless crystalline product, compound **1** (eq 1). Compound **1** was observed to be largely insoluble in water

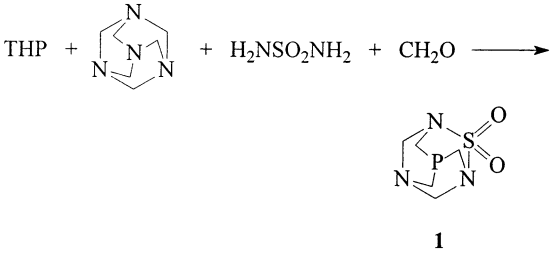

1

(28) SMART 1000 CCD; Bruker Analytical X-ray Systems, Madison, WI, 1999.

(29) SAINT-Plus, version 6.02; Bruker Analytical X-ray Systems, Madison, WI, 1999.

(30) Sheldrick, G. SHELXS-86 Program for Crystal Structure Solution; Institut fur Anorganische Chemie der Universitat, Tammanstrasse 4, D-3400 Gottingen, Germany, 1986.

(31) Sheldrick, G. SHELXL-97 Program for Crystal Structure Refinement; Institut fur Anorganische Chemie der Universitat, Tammanstrasse 4, D-3400 Gottingen, Germany, 1997.

(32) SHELXTL, version 5.0; Bruker Analytical X-ray Systems, Madison, WI, 1999.

(33) Dunning, T. H., Jr.; Hay, P. J. In *Modern Theoretical Chemistry*; Schaefer, H. F., III, Ed.; Plenum: New York, 1976, pp 1−28.

(34) (a) Ditchfield, R.; Hehre, W. J.; Pople, J. A. *J. Chem. Phys.* **1971**, *54*, 724. (b) Hehre, W. J.; Ditchfield, R.; Pople, J. A. *J. Chem. Phys.* **1972**, *56*, 2257. (c) Hariharan, P. C.; Pople, J. A. *Mol. Phys.* **1974**, *27*, 209. (d) Gordon, M. S. *Chem. Phys. Lett.* **1980**, *76*, 163. (e) Hariharan, P. C.; Pople, J. A. *Theor. Chim. Acta* **1973**, *28*, 213.

(35) (a) Becke, A. D. *Phys. Rev. A* **1988**, *38*, 3098. (b) Becke, A. D. *J. Chem. Phys.* **1993**, *98*, 5648.

(36) Lee, C.; Yang, W. *Phys. Rev. B* **1988**, *37*, 785.

(37) Frisch, M. J.; Trucks, G. W.; Schlegel, H. B.; Scuseria, G. E.; Robb, M. A.; Cheeseman, J. R.; Zakrzewski, V. G.; Montgomery, J. A., Jr.; Stratmann, R. E.; Burant, J. C.; Dapprich, S.; Millam, J. M.; Daniels, A. D.; Kudin, K. N.; Strain, M. C.; Farkas, O.; Tomasi, J.; Barone, V.; Cossi, M.; Cammi, R.; Mennucci, B.; Pomelli, C.; Adamo, C.; Clifford, S.; Ochterski, J.; Petersson, G. A.; Ayala, P. Y.; Cui, Q.; Morokuma, K.; Malick, D. K.; Rabuck, A. D.; Raghavachari, K.; Foresman, J. B.; Cioslowski, J.; Ortiz, J. V.; Stefanov, B. B.; Liu, G.; Liashenko, A.; Piskorz, P.; Komaromi, I.; Gomperts, R.; Martin, R. L.; Fox, D. J.; Keith, T.; Al-Laham, M. A.; Peng, C. Y.; Nanayakkara, A.; Gonzalez, C.; Challacombe, M.; Gill, P. M. W.; Johnson, B. G.; Chen, W.; Wong, M. W.; Andres, J. L.; Head-Gordon, M.; Replogle, E. S.; Pople, J. A. *Gaussian 98*, revision A.7; Gaussian, Inc.: Pittsburgh, PA, 1998.

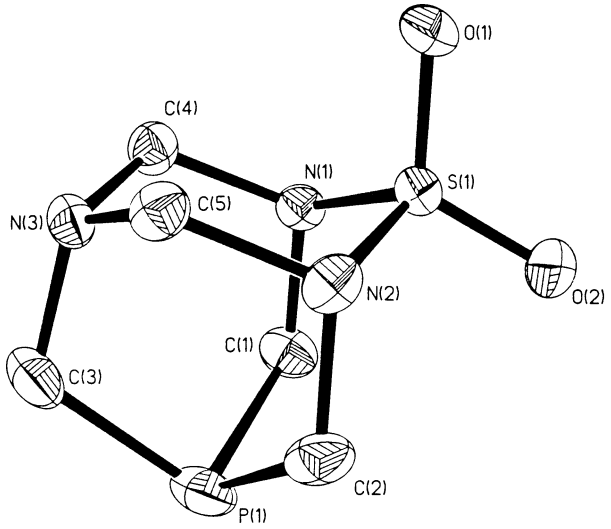

Figure 1. Thermal ellipsoid drawing of compound **1**. Thermal ellipsoids are drawn with 50% probability.

with a solubility of less than 0.70 g/L. Further, attempts to solubilize the compound via protonation in 0.1 M HCl failed as well. Therefore, unlike PTA, $PASO_2$ appears to offer no advantage in the context of serving as a ligand for the preparation of water-soluble organotransition-metal complexes for use in catalysis. However, compound **1** was found to be readily soluble in DMSO and acetone. When the reaction in eq 1 was carried out in the absence of THP, the tetramethylenetetraamine analogue of compound **1**, **2**, was isolated.

Solid-State Characterization of Compounds 1 and 2. X-ray-quality crystals of **1** and **2** were grown as described in the Experimental Section. Crystallographic data and data collection parameters determined at 110 K may be found in Table 1. A thermal ellipsoid drawing of **1** is shown in Figure 1, along with the atomic numbering scheme. Selected bond distances and angles are given in Table 2.

The phosphaadamantane compound **1** is structurally quite similar to PTA, exhibiting obvious differences due to the incorporation of the SO_2 moiety in place of a methylene functionality. Carbon−nitrogen bond distances for nitrogen atoms adjacent to the SO_2 unit are 1.507(2) and 1.496(2) Å for N1−C4 and N1−C6, respectively, and 1.512(2) and 1.497(2) Å for N2−C5 and N2−C8, respectively. Carbon−nitrogen bond distances corresponding to the nitrogen atom distal to the SO_2 unit show statistically significant differences and correspond more closely to those observed for PTA.[38] They are 1.451(2), 1.453(3), and 1.478(3) Å for the N3−C4, N3−C5, and N3−C7 bonds, respectively. The corresponding bond distances reported for PTA are 1.461(4), 1.465(4), and 1.463(3) Å for all three N−C bonds in the asymmetric unit.[38] Thus, the structural implications of incorporation of the SO_2 functionality into the adamantyl structure are at least statistically significant. Further illustration of this can be seen through examination of the C−P−C bond angles. The angle ∠C1−P1−C2 is measured to be 98.03(9)°, while the remaining two angles ∠C1−P1−C3 and ∠C2−P1−C3 are 95.76(10) and 95.55(9)°, respectively. The corresponding C−P−C bond angle in PTA was measured as 96.1(1)° for the only such angle in the asymmetric unit.[38]

Figure 2 contains a thermal ellipsoid representation of **2**, with selected bond distances and angles provided in Table 2. Like its phosphaadamantane analogue, the average carbon−nitrogen bond distance for nitrogen atoms adjacent to the SO_2 unit (N(2) and N(3)) at 1.519(3) Å is slightly longer than the average carbon−nitrogen bond distance corresponding to the nitrogen

Table 2. Selected Bond Distances (Å) and Angles (deg) for Compounds 1−3, 4a, 7, and 8[a]

Complex 1			
P(1)−C(2)	1.858(2)	P(1)−C(3)	1.860(2)
P(1)−C(1)	1.857(2)	N(1)−C−(1)	1.497(2)
N(1)−C(4)	1.512(2)	N(2)−C(2)	1.496(2)
N(2)−C(5)	1.507(2)	N(3)−C(3)	1.478(3)
N(3)−C(4)	1.453(2)	N(3)−C(5)	1.451(2)
C(1)−P(1)−C(2)	98.03(9)	C(1)−P(1)−C(3)	95.76(10)
C(2)−P(1)−C(3)	95.55(9)	C(1)−N(1)−C(4)	111.04(15)
C(2)−N(2)−C(5)	111.41(15)	C(4)−N(3)−C(3)	111.72(16)
C(5)−N(3)−C(3)	111.63(16)	C(4)−N(3)−C(5)	111.01(15)
Compound 2			
N(1)−C(1)	1.471(3)	N(1)−C(2)	1.469(3)
N(1)−C(3)	1.469(3)	N(2)−C(1)	1.514(3)
N(2)−C(4)	1.521(3)	N(3)−C(2)	1.516(3)
N(3)−C(5)	1.524(3)	N(4)−C(3)	1.475(3)
N(4)−C(4)	1.459(3)	N(4)−C(5)	1.457(3)
C(1)−N(1)−C(2)	110.22(17)	C(1)−N(1)−C(3)	108.17(17)
C(2)−N(1)−C(3)	107.90(16)	C(1)−N(2)−C(4)	107.53(18)
C(2)−N(3)−C(5)	108.05(17)	C(4)−N(4)−C(3)	108.71(16)
C(5)−N(4)−C(3)	109.04(17)	C(4)−N(4)−C(5)	110.10(16)
Complex 3			
P(1)−O(3)	1.396(4)	P(1)−C(1)	1.845(3)
P(1)−C(2)	1.847(3)	P(1)−C(3)	1.837(3)
N(1)−C(1)	1.495(3)	N(1)−C(4)	1.510(3)
N(2)−C(2)	1.494(3)	N(2)−C(5)	1.517(3)
N(3)−C(3)	1.481(3)	N(3)−C(4)	1.460(3)
N(3)−C(5)	1.454(3)		
C(1)−P(1)−C(2)	99.96(13)	C(1)−P(1)−C(3)	97.55(12)
C(2)−P(1)−C(3)	98.19(13)	C(1)−N(1)−C(4)	111.0(2)
C(2)−N(2)−C(5)	110.5(2)	C(3)−N(3)−C(4)	111.7(2)
C(3)−N(3)−C(5)	112.05(19)	C(4)−N(3)−C(5)	111.7(2)
Compound 4a			
P(1)−C(1)	1.828(9)	P(1)−C(2)	1.817(9)
P(1)−C(3)	1.814(10)	P(1)−C(6)	1.770(11)
N(1)−C(1)	1.435(14)	N(1)−C(4)	1.520(10)
N(2)−C(2)	1.422(15)	N(2)−C(5)	1.567(12)
N(3)−C(3)	1.453(12)	N(3)−C(4)	1.457(12)
N(3)−C(5)	1.466(12)		
C(1)−P(1)−C(2)	103.7(8)	C(1)−P(1)−C(3)	100.4(8)
C(2)−P(1)−C(3)	102.6(9)	C(1)−P(1)−C(6)	115.6(6)
C(2)−P(1)−C(6)	115.3(6)	C(3)−P(1)−C(6)	117.2(5)
C(4)−N(3)−C(5)	113.0(10)		
Compound 7			
W(1)−C(1)	2.002(6)	W(1)−C(2)	2.068(8)
W(1)−C(3)	2.055(6)	W(1)−C(4)	2.043(8)
W(1)−C(5)	2.048(6)	W(1)−P(1)	2.4976(15)
C(1)−W(1)−P(1)	172.02(17)	C(2)−W(1)−P(1)	94.6(2)
C(3)−W(1)−P(1)	95.47(17)	C(4)−W(1)−P(1)	88.13(17)
C(5)−W(1)−P(1)	83.6(2)		
Compound 8			
W(1)−C(1)	1.992(9)	W(1)−C(2)	2.053(10)
W(1)−C(3)	2.061(11)	W(1)−C(4)	2.067(10)
W(1)−C(5)	2.060(10)	W(1)−P(1)	2.478(3)
C(1)−W(1)−P(1)	172.2(2)	C(2)−W(1)−P(1)	85.9(3)
C(3)−W(1)−P(1)	87.3(3)	C(4)−W(1)−P(1)	94.2(3)
C(5)−W(1)−P(1)	93.03(3)		

[a] Estimated standard deviations are given in parentheses.

(38) Fluck, E.; Forester, J.; Weidlien, J.; Hadicke, E. *Z. Naturforsch., B* **1977**, *32B*, 499.

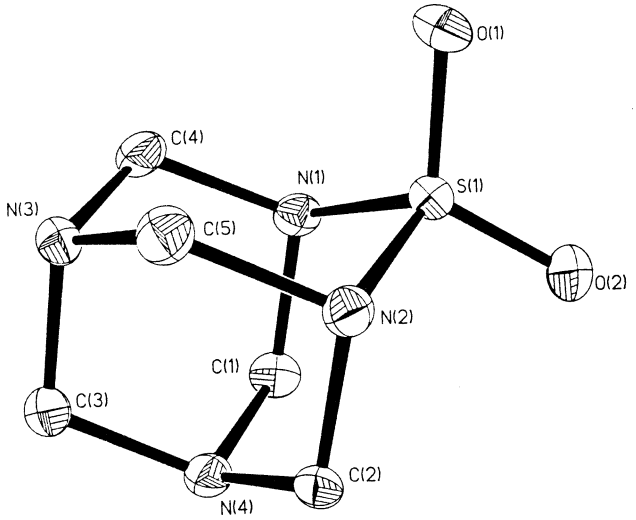

Figure 2. Thermal ellipsoid drawing of compound **2**. Thermal ellipsoids are drawn with 50% probability.

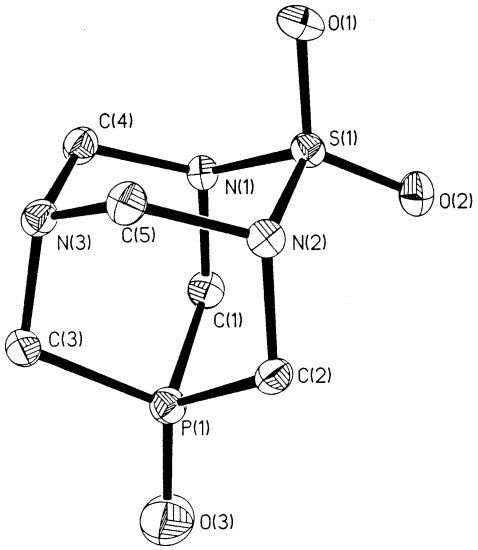

Figure 3. Thermal ellipsoid drawing of compound **3**. Thermal ellipsoids are drawn with 50% probability.

atoms (N(1) and N(4)) distal to the SO_2 moiety of 1.471(3) Å. The average sulfur−nitrogen and sulfur−oxygen bond distances in compound **2**, at 1.657(3) and 1.435(2) Å, are quite similar to those observed in compound **1**.

Solid-State Characterization of Compound 3. Compound **3** was synthesized as described in the literature.[24] Herein we report its crystal structure for the sake of completeness. X-ray-quality crystals of **3** were grown from an acetone solution via slow recrystallization at −10 °C. Crystal data and data collection parameters obtained at 110 K are provided in Table 1. A thermal ellipsoid representation of compound **3** with atomic numbering scheme is shown in Figure 3, with selected bond distances and angles listed in Table 2. The structural features of compound **3** are congruent with those observed in compound **1**. The main differences are those associated with oxidation of the phosphorus; e.g., the P−C bond lengths (average 1.843(3) Å) are slightly shorter than those in compound **1** (ave. 1.858(3)Å).

Synthesis, Spectral, and Solid-State Characterization of Compound 4. Methylation of compound **1** was achieved upon refluxing a slight excess of methyl iodide with a 1:8 (chloroform/ethyl acetate) solution of **1** as described in the literature.[24] The ^{1}H NMR spectrum of compound **4** in D_2O exhibited a doublet centered at 1.97 ppm with a coupling constant of 17.3 Hz (J_{P-CH_3}) (see inset in Figure 4), along with complex signals centered around 5 ppm. These chemical shifts were previously reported by Daigle and support his assignment that methylation had occurred at the phosphorus position.[24] This is in contrast to what is observed upon methylation of PTA with methyl iodide, where methylation occurs at one of the nitrogen positions.[38] The ^{31}P NMR spectrum of **4** in D_2O displayed an intense signals at δ −39.2 ppm, which is also indicative of methylation at phosphorus (Figure 4). Nevertheless, there was an additional weak ^{31}P resonance at δ −109.5 ppm. This second species is suggestive of compound **1** methylated at a nitrogen site; recall that the ^{31}P resonance for PTA in D_2O appears at δ −96 ppm.

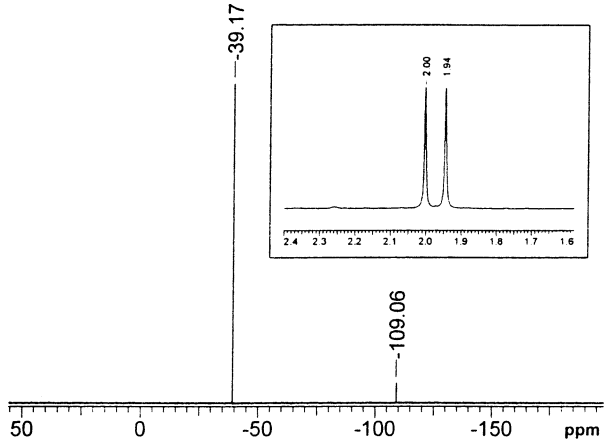

Figure 4. ^{1}H and ^{31}P NMR spectra of the cation of compound **4** in D_2O.

The assignment of the minor component in the ^{31}P NMR spectrum of the methylation reaction of compound **1** to a nitrogen-methylated derivative of $PASO_2$ is further supported by crystallographic analysis. X-ray-quality crystals of compound **4** were grown by slow evaporation from an aqueous solution. Data collection parameters and crystallographic data at 110 K are given in Table 1. The initial refinement was carried out with assignment of phosphorus at the methylated position. Given this interpretation, two atom types were refined at each of the ambiguous sites, phosphorus and nitrogen. This was then refined to a final R value of 3.54%. Figure 5 shows a thermal ellipsoid drawing of the major component that was methylated at phosphorus, along with the atomic numbering scheme. The top inset shows a ball-and-stick drawing of both components as they appear in the crystal structure. It is here that the nature of the internal disorder is most clearly illustrated. The lower inset shows a thermal ellipsoid drawing of the second species, that methylated at the nitrogen site. Selected bond distances and angles are given in Table 2. Final values for the refined component ratios for the phosphorus−nitrogen pairs are, on average, 2:3 for methylated nitrogen to methylated phosphorus. However, the NMR data are much more representative of the product composition; i.e., integration of the ^{31}P NMR spectrum of compound **4** gives a ratio of 1:4, as shown in Figure 4.

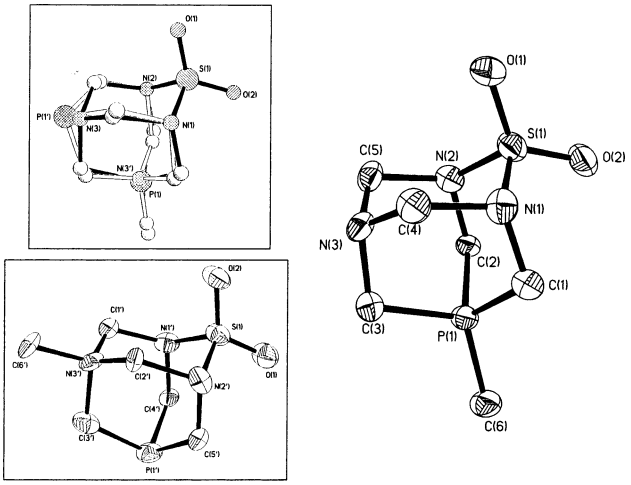

Figure 5. Thermal ellipsoid drawing of the major component of the cation of compound **4**, with insets giving a ball-and-stick drawing of both components as well as a thermal ellipsoid drawing of the minor component. Thermal ellipsoids are drawn with 50% probability.

Table 3. Selected Structural Parameters of Compound 1[a]

	theoretical		
	DFT	HF	exptl
P(1)−C(1)	1.903	1.883	1.857(2)
P(1)−C(2)	1.903	1.883	1.858(2)
P(1)−C(3)	1.900	1.880	1.860(2)
N(1)−C(1)	1.487	1.477	1.497(2)
N(1)−C(4)	1.497	1.480	1.512(2)
N(2)−S(1)	1.718	1.663	1.6437(17)
N(3)−C(3)	1.472	1.462	1.478(3)
N(3)−C(4)	1.462	1.451	1.453(3)
N(3)−C(5)	1.462	1.451	1.451(2)
C(1)−P(1)−C(2)	97.6	97.778	98.03(9)
C(1)−P(1)−C(3)	94.5	95.262	95.76(10)
C(2)−P(1)−C(3)	94.5	95.263	95.55(9)
C(1)−N(1)−C(4)	112.3	112.506	111.04(15)
C(2)−N(2)−C(5)	112.3	112.511	111.41(15)
C(4)−N(3)−C(5)	110.7	110.759	111.01(15)
C(3)−N(3)−C(4)	112.1	112.203	111.72(16)
C(3)−N(3)−C(5)	112.1	112.205	111.63(16)

[a] All distances are given in angstroms and all angles are given in degrees. Estimated standard deviations are given in parentheses.

Theoretical Computations. In an effort to gain some insight into the disparity in the sites of alkylation activity of PTA and $PASO_2$, we have performed ab initio computations on these two compounds. As has been outlined thus far, PTA exhibits preferential alkylation at one of the three nitrogen sites, while $PASO_2$ exhibits preference at the phosphorus site. It was anticipated that calculations would provide information as to electronic changes or differences associated with incorporation of SO_2 moiety into the adamantane-like structure.

Geometry optimizations were carried out on compounds **1**, **4a**,**b**, **5**, and **6a**,**b** using ab initio methods, as described in the Experimental Section. The optimizations produced parameters consistent with the known structure of $PASO_2$, as shown in Table 3. First, investigations into the charge distributions were carried out to determine whether the phosphorus atom exhibited more negative charge relative to the nitrogen atoms in $PASO_2$, a characteristic not expected to be shared by PTA. However, as can be readily seen in Figure 6, the

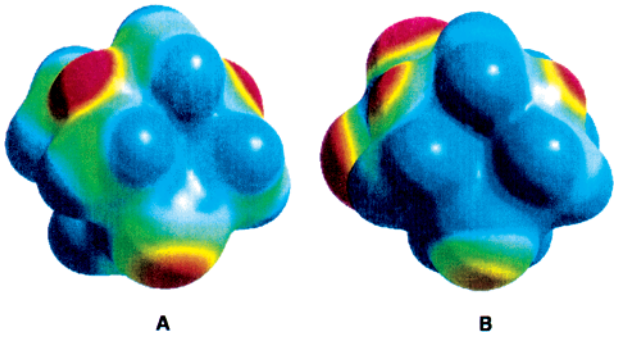

Figure 6. Charge distributions in (a) PTA (**5**) and (b) $PASO_2$ (**1**).

distribution showed a somewhat smaller region of negative charge associated with the phosphorus site for $PASO_2$ relative to that shown for PTA. Also, examination and comparison of the frontier orbitals for PTA and $PASO_2$ provided no obvious answers to the current question.

Another possibility we chose to investigate was product stability. Therefore, through modification of the optimized $PASO_2$ structures, the alkylated species **4a**,**b** and **6a**,**b** were obtained. Optimizations were carried out on these four structures as described previously, and on the basis of the single-point energies calculated for these new structures, it was shown that the most stable product was that methylated at the nitrogen atom for both PTA and $PASO_2$. Having exhausted all other possibilities, it is apparent that the reactions in question are directed by the nature of the transition states. Unfortunately, we have not performed calculations on possible transition states in the methylation of PTA or $PASO_2$ and as a consequence can offer no details in this area.

Synthesis, Spectral Properties, and X-ray Structures of Complexes 7 and 8. In an effort to assess the nature of $PASO_2$ as a ligand, complexes **7** and **8** were prepared from the reaction of PTA or $PASO_2$ and $(CO)_5W(N(CH_3)_3)$ as described in the Experimental Section. Both complexes were analyzed by IR spectroscopy. The patterns observed in the ν(CO) region of each spectrum are typical of singly substituted octahedral metal carbonyls of approximate C_{4v} symmetry. The synthesis and spectroscopic characterization have been reported previously for complex **7**, along with other group 6 metal PTA pentacarbonyl derivatives.[39] Comparison of the ν(CO) stretching frequencies for **7** (2072 ($A_1^{(2)}$), 1955 ($A_1^{(1)}$), and 1944 cm^{-1} (E)) and **8** (2077, 1950 (sh), and 1945 cm^{-1}) reveal the two phosphines to be quite similar in electronic character. This is further illustrated by the corresponding Cotton−Kraihanzel carbonyl force constants calculated from these data, where the calculated values for k_1, k_2, and k_i are 15.65_7, 15.89_1, and 0.31 in **7** and 15.58_6, 15.92_7, and 0.32 in complex **8**.[40] In both metal derivatives, significant downfield ^{31}P NMR chemical shifts are observed upon binding of the ligand: i.e., for complex **7** in DMSO δ −78.2 ppm ($J^{183}_{W-^{31}P}$ = 218.2 Hz) vs −97.96 ppm for the free PTA ligand, and for complex **8** in DMSO δ −81.56

(39) Darensbourg, M. Y.; Daigle, D. J. *Inorg. Chem.* **1975**, *14*, 1217.
(40) Cotton, F. A.; Kraihanzel, C. S. *J. Am. Chem. Soc.* **1962**, *84*, 4432.

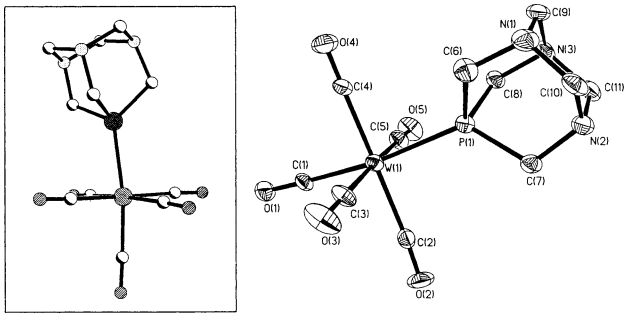

Figure 7. Thermal ellipsoid drawing of complex **7**. The insert illustrates the tilt of the PTA ligand in complex **7** relative to the axial W−CO grouping. Thermal ellipsoids are drawn with 50% probability.

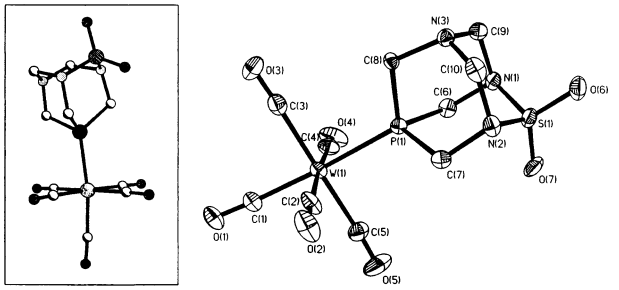

Figure 8. Thermal ellipsoid drawing of complex **8**. The insert illustrates the tilt of the PTA ligand in complex **8** relative to the axial W−CO grouping. Thermal ellipsoids are drawn with 50% probability.

ppm ($J^{183}_{W-^{31}P}$ = 228.9 Hz) vs −115.9 ppm for the free phosphine.

Yellow crystals of these complexes were obtained from the slow evaporation of a hexane solution or crystallization at −10 °C. Using these samples, single-crystal X-ray diffraction experiments were conducted. Crystal data and data collection parameters are given in Table 1. A thermal ellipsoid drawing of **7** is shown in Figure 7. Selected bond distances and angles are given in Table 2. Complex **7** crystallized into the monoclinic space group $P2_1/c$. The tungsten center exhibits slightly distorted octahedral coordination with C−M−C bond angles varying from 86.5(3) to 94.6(2)°. Further, there are two distinctly different M−CO bond distances. The axial W(1)−C(1) bond, trans to PTA, is observed to have a significantly shorter bond distance than those of the other four equatorial carbonyls. These are measured to be 2.002(6), 2.068(8), 2.055(6), 2.043(8), and 2.048(6) Å, for the W(1)−C(1), −C(2), −C(3), −C(4), and −C(5) bonds, respectively. The PTA ligand is oriented such that the P−C(7) bond bisects the equatorial C(4)−W(1)−C(3) bond angle, while the other two P−C bonds adopt a somewhat eclipsed orientation relative to the equatorial W(1)−C(2) and W(1)−C(5) bonds. Another, not entirely unusual, observation is that the PTA ligand exhibits a pronounced tilt relative to the W(1)−C(1)−O(1) axis, as seen in the inset to Figure 7. This has been reported in the past for other phosphine complexes of the group 6 pentacarbonyls[41−44] and has also been seen for the analogous $Mo(CO)_5$PTA complex,[45] although it is not quite as pronounced as this case.

Generally, the structural data obtained for **8** were quite similar to those seen for **7**. Crystallographic data and data collection parameters are given in Table 1. A thermal ellipsoid drawing is shown in Figure 8. Selected bond distances and angles are given in Table 2. Complex **8** crystallized in the monoclinic space group $P2_1/c$. The coordination geometry was observed to be slightly distorted octahedral, as in the case of **7**. Further, as was the case for **7**, the axial W−CO bond distance was observed to be the shortest of the W−C bonds, which are measured to be 1.992(9), 2.053(10), 2.061(11), 2.067(10), and 2.060(10) Å for the W(1)−C(1), −C(2), −C(3), −C(4), and −C(5) bonds, respectively. Compounds **7** and **8** were observed to have very similar W−P bond distances as well: 2.4976(15) and 2.478(8) Å for **7** and **8**, respectively. As is clear from the drawing in Figure 8, **8** is observed to exhibit a tilt relative to the W(1)−C(1)−O(1) axis, as was the case for complex **7**. This is evident from the W−P−C bond angle data, which are 123.1(3), 117.1(3), and 116.5(3)° for the W(1)−P(1)−C(6), −C(7), and −C(8) angles, respectively.

Concluding Remarks

While it is unmistakable that, without further derivatization, $PASO_2$ offers no utility as a water-soluble ligand, it is an interesting example of a sterically unencumbering, aliphatic phosphine. Further, while it was observed to behave very differently from PTA, in terms of both its solubility and alkylation reactions, it was clearly very similar in electronic character and coordination chemistry, as evidenced by the IR, NMR, theoretical calculation, and X-ray crystallographic results, presented for complexes **7** and **8**. The most striking difference were the products observed for the alkylation reactions with methyl iodide. While it was generally accepted that PTA is only alkylated at one of its three nitrogen atoms, $PASO_2$ was observed to produce predominantly a phosphonium salt upon alkylation. This prompted us to reexamine the PTA alkylation reaction more closely, and with the discovery of a small fraction of the product in the phosphonium form, it is quite clear that the competition for alkylation between nitrogen and phosphorus in PTA is not quite as unambiguous as previously thought. Given the similarities between the two tertiary phosphines, it is reasonable to assert that subtle differences in the electronic and steric character about the phosphorus center lead to significant differences in the relative rates of alkylation at the nitrogen and phosphorus sites.

Acknowledgment. Financial support from the National Science Foundation (Grant Nos. CHE-99-10342 and CHE 98-07975, with the latter being for the purchase of X-ray equipment), and the Robert A. Welch Foundation is greatly appreciated.

Supporting Information Available: Complete details of the X-ray diffraction studies on compounds **1**−**3**, **4a**,**b**, **7**, and **8**. This material is available free of charge via the Internet at http://pubs.acs.org.

OM0300225

(41) Davies, M. S.; Aroney, M. J.; Buys, I. E.; Hambley, T. W. *Inorg. Chem.* **1995**, *34*, 330.
(42) Lee., K. J.; Brown, T. L. *Inorg. Chem.* **1992**, *31*, 289.
(43) Cotton, F. A.; Darensbourg, D. J.; Ilsley, W. H. *Inorg. Chem.* **1981**, *20*, 578.
(44) Cotton, F. A.; Darensbourg, D. J.; Kolthammer, B. W. S. *Inorg. Chem.* **1981**, *20*, 4440.
(45) Delerno, J. R.; Trefonas, L. M.; Darensbourg, M. Y.; Majeste, R. J. *Inorg. Chem.* **1976**, *15*, 816.